

**AFRL-ML-WP-TR-2003-4011**

**LASER CLADDING ON CARBON-CARBON COMPOSITES**



**Major John J. Eric**

**Structural Materials Branch (AFRL/MLBC)  
Nonmetallic Materials Division  
Materials and Manufacturing Directorate  
Air Force Research Laboratory, Air Force Materiel Command  
Wright-Patterson Air Force Base, OH 45433-7750**

**Robert J. Hull**

**Anteon Corporation  
5100 Springfield Pike, Suite 509  
Dayton, OH 45431-1264**

**DECEMBER 2002**

**Final Report for 14 December 1998 – 15 August 2000**

**Approved for public release; distribution is unlimited.**

**MATERIALS AND MANUFACTURING DIRECTORATE  
AIR FORCE RESEARCH LABORATORY  
AIR FORCE MATERIEL COMMAND  
WRIGHT-PATTERSON AIR FORCE BASE, OH 45433-7750**

**NOTICE**

Using government drawings, specifications, or other data included in this document for any purpose other than government procurement does not in any way obligate the US Government. The fact that the government formulated or supplied the drawings, specifications, or other data does not license the holder or any other person or corporation or convey any rights or permission to manufacture, use, or sell any patented invention that may relate to them.

This report is releasable to the National Technical Information Service (NTIS). At NTIS, it will be available to the general public, including foreign nations.

This technical report has been reviewed and is approved for publication.

  
\_\_\_\_\_  
JOHN J. ERIC, Major, USAFR  
Structural Materials Branch  
Nonmetallic Materials Division

  
\_\_\_\_\_  
TIA BENSON TOLLE, Chief  
Structural Materials Branch  
Nonmetallic Materials Division

  
\_\_\_\_\_  
ROBERT M. SUSNIK, Deputy Chief  
Nonmetallic Materials Division  
Materials and Manufacturing Directorate

Do not return copies of this report unless contractual obligations or notice on a specific document requires its return.

<b>REPORT DOCUMENTATION PAGE</b>				<i>Form Approved</i> <i>OMB No. 0704-0188</i>	
<small>The public reporting burden for this collection of information is estimated to average 1 hour per response, including the time for reviewing instructions, searching existing data sources, gathering and maintaining the data needed, and completing and reviewing the collection of information. Send comments regarding this burden estimate or any other aspect of this collection of information, including suggestions for reducing this burden, to Department of Defense, Washington Headquarters Services, Directorate for Information Operations and Reports (0704-0188), 1215 Jefferson Davis Highway, Suite 1204, Arlington, VA 22202-4302. Respondents should be aware that notwithstanding any other provision of law, no person shall be subject to any penalty for failing to comply with a collection of information if it does not display a currently valid OMB control number. PLEASE DO NOT RETURN YOUR FORM TO THE ABOVE ADDRESS.</small>					
<b>1. REPORT DATE (DD-MM-YY)</b> December 2002		<b>2. REPORT TYPE</b> Final		<b>3. DATES COVERED (From - To)</b> 12/14/1998 – 08/15/2000	
<b>4. TITLE AND SUBTITLE</b> LASER CLADDING ON CARBON-CARBON COMPOSITES				<b>5a. CONTRACT NUMBER</b> In-house	
				<b>5b. GRANT NUMBER</b>	
				<b>5c. PROGRAM ELEMENT NUMBER</b> 61102F	
<b>6. AUTHOR(S)</b> Major John J. Eric (AFRL/MLBC) Robert J. Hull (Anteon)				<b>5d. PROJECT NUMBER</b> 4347	
				<b>5e. TASK NUMBER</b> 2P	
				<b>5f. WORK UNIT NUMBER</b> IO	
<b>7. PERFORMING ORGANIZATION NAME(S) AND ADDRESS(ES)</b> Structural Materials Branch (AFRL/MLBC) Nonmetallic Materials Division Materials and Manufacturing Directorate Air Force Research Laboratory, Air Force Materiel Command Wright-Patterson Air Force Base, OH 45433-7750				<b>8. PERFORMING ORGANIZATION REPORT NUMBER</b>  AFRL-ML-WP-TR-2003-4011	
<b>9. SPONSORING/MONITORING AGENCY NAME(S) AND ADDRESS(ES)</b> Materials and Manufacturing Directorate Air Force Research Laboratory Air Force Materiel Command Wright-Patterson AFB, OH 45433-7750				<b>10. SPONSORING/MONITORING AGENCY ACRONYM(S)</b> AFRL/MLBC	
				<b>11. SPONSORING/MONITORING AGENCY REPORT NUMBER(S)</b> AFRL-ML-WP-TR-2003-4011	
<b>12. DISTRIBUTION/AVAILABILITY STATEMENT</b> Approved for public release; distribution is unlimited.					
<b>13. SUPPLEMENTARY NOTES</b> Report contains color.					
<b>14. ABSTRACT</b> This report describes the results of experiments on laser cladding a variety of protective coatings onto carbon-carbon substrates as oxidation-protection coatings. The work was performed using a 12-kW flattop CO <sub>2</sub> laser and a powder delivery system to inject the material to be deposited into the laser beam at the surface of the sample to be coated. The laser beam is delivered by a series of optics to the substrate, where it is focused to an approximately 1.3-cm-diameter spot size. Most of the test cases used 6 kW/cm <sup>2</sup> to clad the coating material to the substrate surface. Coating materials included powdered aluminum, nickel chromium alloy, gray alumina ceramic, and a magnesium oxide/zirconium oxide ceramic. Mixed results were obtained, with the alumina providing a slightly better cladding, based on visual appearance and micrographic views.					
<b>15. SUBJECT TERMS</b> carbon-carbon, laser cladding, oxidation protection, protective coatings					
<b>16. SECURITY CLASSIFICATION OF:</b>			<b>17. LIMITATION OF ABSTRACT:</b> SAR	<b>18. NUMBER OF PAGES</b> 50	<b>19a. NAME OF RESPONSIBLE PERSON (Monitor)</b> Major John J. Eric <b>19b. TELEPHONE NUMBER (Include Area Code)</b> (937) 255-3808 x3165
<b>a. REPORT</b> Unclassified	<b>b. ABSTRACT</b> Unclassified	<b>c. THIS PAGE</b> Unclassified			

## TABLE OF CONTENTS

	<u>PAGE</u>
1.0 Introduction .....	1
2.0 Background .....	2
3.0 Laser Cladding at LHMEEL .....	3
3.1 Experimental Setup .....	4
3.2 Samples to be Coated .....	7
3.3 Sample Coating Runs.....	8
3.3.1 Series 1—Toward the Coating of Aluminum on C-C.....	8
3.3.1.1 Setup Confirmation Tests .....	8
3.3.1.2 First Aluminum Trials.....	9
3.3.1.3 Reintroduction of Powder Feeder.....	11
3.3.1.4 Powder Feed Using Fine Powder Nozzle .....	12
3.3.1.5 C-C Trials .....	14
3.3.1.6 Program C-C Sample Testing (Contractor’s Samples) .....	19
3.3.2 Test Review Meeting .....	24
3.3.3 Initial Micrographic Review of Selected Samples .....	24
3.3.4 Summary Micrographic Data Review.....	26
3.3.5 Series 2—Tests on a Common C-C Substrate .....	28
3.3.5.1 Nickel on Steel Substrate .....	30
3.3.5.2 Nickel on C-C Substrate .....	30
3.3.5.3 Alumina on C-C Substrate.....	32
3.3.5.4 Magnesium Oxide/Zirconium Oxide on C-C Substrate .....	32
3.3.6 Discussion of Series 2 Preliminary Results .....	33
3.3.7 Summary Discussion of Micrograph Results .....	35
4.0 Summary .....	38
5.0 References .....	39

## LIST OF FIGURES

<u>FIGURE</u>		<u>PAGE</u>
1	Target Substrate Location .....	5
2	Sample Holder in Containment Box.....	5
3	Full View of Cladding Apparatus .....	6
4	Sample P71: Versalloy on Steel .....	9
5	Sample P83: Aluminum on Graphite .....	11
6	Samples P9 (left) and P92 (right): Aluminum on Steel .....	14
7	Sample P95: Aluminum on Steel.....	16
8	Sample P99: Aluminum on C-C.....	16
9	Sample P100: Aluminum on C-C.....	17
10	Sample P101: Aluminum on C-C Thermal Plane Material.....	18
11	Sample P102: Aluminum on Larger C-C Thermal Plane Material.....	18
12	Sample P103: Aluminum on Nondensified C-C .....	20
13	Sample P104: Aluminum on Thin, Dense C-C .....	21
14	Sample P105: Aluminum on Aluminized, Machined C-C.....	21
15	Sample P106: Aluminum on Aluminized, Machined C-C.....	23
16	Sample P107: Aluminum on Aluminized C-C .....	23
17	Cracking Below Surface of Sample P100, Run #1 .....	27
18	Aluminum/C-C Interface on Sample P102, Run #1 .....	27
19	Aluminum Penetration Into Surface of Sample P102, Run #1 ...	27
20	Aluminum Clad Follows the Machined Features on Sample P105.....	28
21	Aluminum Clad Over a Machined Feature on Sample P106 .....	29
22	Aluminum Cladding on a Machined Feature on Sample P106 ..	29
23	View Further Down the Side of Figure 22 Feature (P106).....	29
24	Nickel Chromium Alloy Clad on Steel.....	31
25	Nickel Alloy Cladding Using Bi-Directional Passes.....	31
26	Nickel Alloy Cladding Using Single-Direction Rastering .....	31

## LIST OF FIGURES (cont'd)

<u>FIGURE</u>		<u>PAGE</u>
27	Grey Alumina Cladding on C-C Using Single-Direction Passes.....	33
28	Magnesium Oxide/Zirconium Oxide on C-C Substrate .....	34
29	Edge View of the Sample Shown in Figure 28 .....	34
30	Alumina Powder Clad Over NiCr Alloy on C-C Substrate.....	35
31	Micrograph of Alumina Cladding on C-C Substrate .....	36
32	Micrograph Showing NiCr Alloy Clad Over a C-C Substrate .....	36
33	Alumina Cladding Over a NiCr-Clad C-C Substrate .....	37

## 1.0 INTRODUCTION

Carbon-carbon (C-C) composite materials—carbon fibers surrounded by a carbon matrix—offer the materials industry a unique mixture of high strength and high temperature performance in a lightweight package. While the aerospace industry has been very interested in C-C for many years for an assortment of high temperature applications, commercial applications for this material are beginning to gain interest and acceptance. One drawback of the C-C composite is its susceptibility to oxidation in nonvacuum environments. A number of studies are underway to investigate thin coatings that can be applied to C-C to reduce or eliminate this oxidation effect.

This report will describe the results of experiments on the laser cladding of a variety of protective coatings onto C-C substrates as potential oxidation-protection coatings. This work, performed using a 12-kW flattop CO<sub>2</sub> laser and a powder delivery system, will be presented. Laser cladding parameters as well as the resulting materials characterizations will be discussed. This work was performed as a project under the AFRL Reserve Program, while assigned to the Structural Materials Branch (AFRL/MLBC), Nonmetallic Materials Division. Assistance in performing the laser cladding series was provided by Mr. Rob Hull and Mr. John Bagford of the Anteon Corp., on-site contractor for the Laser Hardened Materials Evaluation Laboratory (LHMEL) in the Hardened Materials Branch (AFRL/MLPJ), Survivability and Sensor Materials Division. Dr. Dave Anderson and Mr. Bill Ragland of the University of Dayton Research Institute (UDRI), on-site contractor for MLBC, also provided analytical support and laboratory sample preparation instruction.

## 2.0 BACKGROUND

Carbon-Carbon composites (CCC) have been finding increased use in many aerospace applications in recent years. Such properties as their light weight, high thermal conductivity, and high strength make CCCs attractive materials. However, there are some limitations and concerns when CCCs are used in certain environments. Oxidation protection at high temperatures has initiated a search for coating materials that will protect the CCC substrate, yet not inhibit performance of the materials in their intended application.

The interest in coating CCCs with alternative protective coatings was introduced by two separate occurrences. MLBC had programs driven by a long-standing interest in preventing oxidation of the C-C substrate material. The goal of some of these efforts was to look for a way to coat the C-C substrate and prevent an infiltration of the material that would lead to oxidation conditions. The second circumstance that led to this project was the experience that MLPJ's LHMEEL gained in support of pollution-prevention programs investigating chromium replacement techniques and laser-based coating technologies. The result was an interest on the part of both organizations as well as with Anteon in exploring the potential for a laser-based coating process to deposit a protective coating onto a CCC substrate. Metallic and nonmetallic coatings were investigated. The coating, if found to be continuous, would serve as an oxidation barrier for the substrate and demonstrate the feasibility of laser-based coating processes for this application. A metallic coating might also be used to serve as a means to maintain conductivity in electrical or thermal plane applications.

### 3.0 LASER CLADDING AT LHMEL

The laser-based coating effort at LHMEL started as a development program funded by the Air Force Pollution Prevention Office as a means to replace electroplated chrome on Air Force systems such as landing gear elements. As the main Air Force applications for chrome are in the areas of corrosion protection and rebuilding worn surfaces, the replacement metal would have to have properties that include high hardness, low friction, resistance to wear and corrosion, and good surface appearance. The LHMEL effort focused on depositing nickel-based alloys onto a variety of steel substrates. Two approaches were used for the deposition process—laser glazing and laser cladding.

In laser glazing, the high surface heating effect of the laser is used to melt and reflow coatings deposited on a substrate by some other means such as high velocity oxygen-fueled processes, or flame spraying. Since this deposition technique tends to put down a coating that is nonuniform and porous, the laser glazing step serves to establish a continuous, uniform layer with good adherence to meet the requirements for corrosion protection and surface quality.

The laser cladding process in a sense combines the steps of powder deposition and surface processing into one operation. The metal coating material is applied using a powder feeder mechanism and is deposited at the point that a laser beam meets this powder spray incident to the surface of the substrate. The laser energy heats, melts, and applies a uniform, nonporous, and well-bonded coating of the metal onto the substrate. LHMEL has established an in-house laser cladding capability as a result of this previous pollution prevention program and has successfully demonstrated cladding flat surfaces. Since the objective of the CCC coating effort is to investigate a means to deposit a uniform, nonporous protective coating onto a composite, the use of the existing laser cladding apparatus at LHMEL was selected.

### **3.1 Experimental Setup**

The testing done under this effort was conducted in MLPJ's LHMEL, using the LHMEL I laser as the energy source. LHMEL I is a 12-kW CO<sub>2</sub> electrical discharge laser, operated in continuous wave mode at 10.6-micron wavelength. It has a flattop beam profile, which is ideal for materials interaction investigations and for uniform heating of surfaces, as is needed in this application. The beam is delivered by a series of optics to the substrate, where it is focused to an approximately 1.3-cm-diameter spot size. At 6 kW/cm<sup>2</sup> for most of the tests conducted in this series, a front surface temperature of approximately 4000°F was produced at the substrate. The samples, all flat pieces of CCC, are placed one at a time on a graphite block in the center of an aluminum pan (see Figure 1). The pan is mounted on a stage fixed to a translation (CNC) table that can provide x-y movement based on preprogrammed settings. The sample is then enclosed by an aluminum box (see Figure 2) for powder containment. One end of the box is open and has a Plexiglas wall clamped to it for ease of sample observation and video coverage during the deposition process. The top of the box is covered with another graphite plate with a beam entry aperture at the center, again to contain powder as it is applied to the substrate. The box is maintained under a positive purge pressure using Argon gas to enable a clean environment and to reduce the potential for oxidation during the deposition process. Also visible in Figure 2 is the powder feed nozzle at the end of the nozzle arm and powder feed tubing. This enables the powder to be delivered from the powder hopper at the feed apparatus to the sample at a controlled rate. The rate is preset at the powder feed mechanism, and a vibration device in the hopper ensures that a continuous flow of powder is delivered to the nozzle and the sample surface. A complete view of the sample end of the experiment setup is shown in Figure 3.

The powder is delivered to the sample using a Sulzer Metco Type 4MP Powder Feed Unit. According to the device documentation<sup>1</sup>, the 4MP is a self-contained unit employing a fluidized bed design that uses gravity, vibration of the

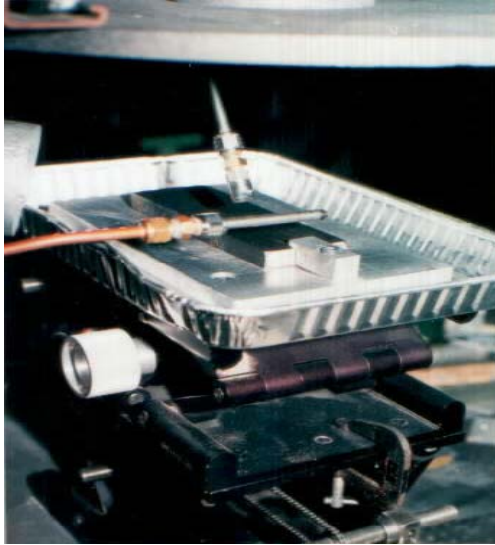


**Figure 1. Target Substrate Location.**

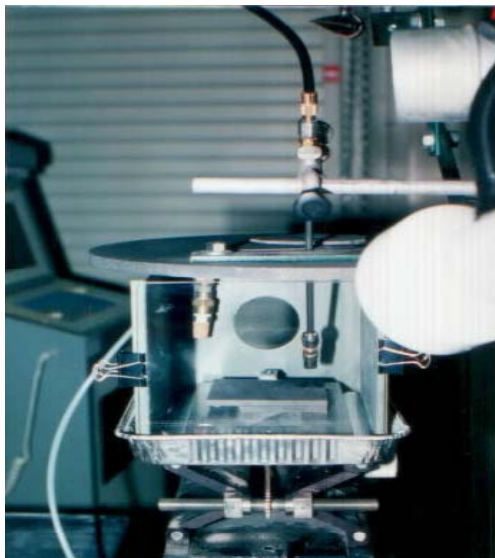


**Figure 2. Sample Holder in Containment Box.**

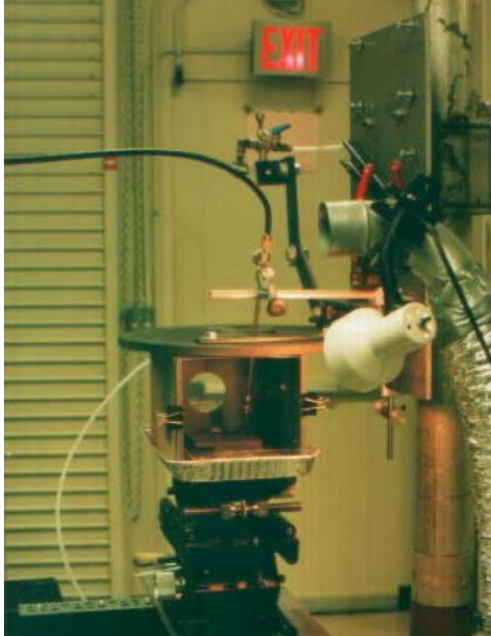


**Figure 3. Full View of Cladding Apparatus.**

powder hopper, and a pressurized gas. The powder is fluidized through the vibration of the hopper, then injected at a controlled rate into the pressurized gas stream. This mechanism serves to provide a constant stream of powder that is then fed through the powder-carrying hose to the feed nozzle (powder port), where it is directed to the substrate surface. The incident laser heats both the substrate and the powder, depositing a coating of the material onto the sample substrate.

For the deposition of the source powder on the substrate, the general procedure calls for the sample to be translated by the table in a single direction under the powder feed nozzle. This is usually programmed as a single pass along one length of the sample substrate. As the sample passes under the nozzle, the powder is sprayed onto the substrate surface. The angle of the nozzle is such that the powder fed from it is placed into the spot of the incident laser beam, which arrives through the aperture in the top plate of the sample box. As the powder enters the beam spot, the laser energy heats it and causes it to melt, thereby, coating the substrate as it passes. Once the programmed pass has been completed, the laser is shut down and the sample is allowed to cool.

The process can be repeated on a single substrate sample, provided sufficient surface area exists for multiple passes to be made without material overlap.

### **3.2 Samples to be Coated**

The project began with five samples of processed CCCs obtained from Applied Material Technologies (AMT), who was under contract with MLBC as part of their advanced development program. The samples included both porous and densified CCCs, and a CCC sample that had been “aluminized” by infiltration of aluminum metal into the composite’s pores, thus, further densifying the material. The purpose of the AMT program was to find a metal-coated CCC material that could serve as a base material for electronic circuitry, with the metal coating providing two major functions. The coating would have to first seal the surface of the CCC, preventing infiltration of oxygen into the structure, and then its inherent electrical conductivity would be used to prevent the buildup of static charge. Thus, the applied coating would have to be thin, uniform, continuous, and conductive. The laser cladding process at LHMEEL was selected to investigate the potential of this technique to provide an effective and inexpensive coating process alternative. Powdered aluminum was used to coat this first set of samples.

After the initial test series, conducted during the period 14 December 1998 through 12 February 1999, a second test series was planned in May 2000 that would incorporate a more uniform set of samples in terms of their pedigree and properties. The samples to be coated in this final series were all cut from two larger 12” x 12” panels of C-C from the same manufacturing lot. The material is a T-300 carbon fiber prepregged with 134A phenolic resin filled with a high purity carbon black.<sup>2</sup> It has 3K tow fibers in an 8HS fiber weave. The bulk density of these panels is on the average 1.75 g/cm<sup>3</sup>. The panels were cut into approximately 2” x 4” coupons, providing a set of consistent samples for the coating runs. Coating trials on these substrates were made using three different powdered materials, all obtained from Sulzer Metco for use with their powder

feed apparatus. The first is a nickel chromium alloy (METCO 43C, 43C-NS) that is primarily a 78% nickel/19% chromium composition.<sup>3</sup> The second is a gray alumina ceramic powder (METCO 101, 101NS, AMDRY 6200), which has 95% Al<sub>2</sub>O<sub>3</sub> and 3% TiO<sub>2</sub>.<sup>4</sup> The final material for this test series is a magnesium oxide/zirconium oxide ceramic powder (METCO 210, 210NS, AMDRY 333), having 76% ZrO<sub>2</sub> and 22% MgO.<sup>5</sup> The primary objective for this test series was to make a best effort at determining the feasibility of depositing these types of materials on a composite substrate by means of laser cladding.

### **3.3 Sample Coating Runs**

#### **3.3.1 Series 1—Toward the Coating of Aluminum on C-C**

##### **3.3.1.1 Setup Confirmation Tests**

The very first set of tests performed were to essentially repeat previous tests of the laser cladding process to make sure that the apparatus was setup and performing properly. This was done by cladding Versalloy 50 (a nickel-based coating) on AISI 1018 Steel. Samples P70 through P75 were processed with some of the deposition parameters varying from run to run to obtain data on the effect these changes would have on the resulting clad. Sample P71 (Figure 4) is the best representative of this series, showing a nice, even clad with good edges through the four passes programmed for this shot. The result matched and is representative of some of the best of the previous cladding experiments performed with this apparatus.

Some of the parameter changes investigated included changing the translation speed of the sample, changing the powder feed rate, and changing the angle of the spray nozzle. For this series of tests, increasing the translation speed did not seem to make much difference, as a good thin coating was still obtained. However, slower speeds tended to leave a much thicker coating which was prone to cracking as the sample cooled. Increasing the feed rate from 25 g/min to 48 g/min seemed to still provide a good coating. However, when the rate jumped to the level of 64 g/min, the coating was again too thick and



**Figure 4. Sample P71: Versalloy on Steel.**

exhibited cracking, even with the original translation speeds. One change that did remain was the change in nozzle angle from 65° to 40°. This removed the nozzle tip from more direct exposure to reflected laser irradiation from the sample surface, protecting the part from physical damage.

#### **3.3.1.2 First Aluminum Trials**

Once the previously achieved cladding performance was re-established, the change was made to aluminum on metal. For this next series, a Metco 99% pure aluminum powder was to be clad on the same steel as from the previous tests. Samples P76 through P86 were used for a total of 20 laser shots during this session. Problems were encountered right from the start. On sample P76, the bar supplying the argon purge was melted; and even at a rate of 20 g/min, there was powder everywhere in the containment box. For the next three runs, using samples P77 and P78, the powder spray was discontinued. Instead, the aluminum powder was prepped by hand in an approximately 1/16" layer on the surface of the substrate. The laser was then directed onto the translating sample in order to melt the metal in a glazing process onto the substrate surface. Initial results showed a rough surface, with the aluminum showing signs of "balling up"

as the laser passes continued. Even when the laser intensity was reduced from  $5 \text{ kW/cm}^2$  to  $2.5 \text{ kW/cm}^2$ , a similar effect was observed. Little improvement was seen in the next two shots, with large “b-b’s,” or balls of aluminum, forming that were very loosely bonded to the substrate. One could easily dislodge these balls with the tip of a pen or using a fingernail. At this point, a decision was made to change the substrate material, in the hopes that the surface heating characteristics of a substrate closer to the objective material would improve the melting and adhesion of the powdered metal.

The first “new” substrate material tried was carbon phenolic on sample P81. This material did not fare well, as it started to burn off the phenolic and a large amount of smoke was created. Another change was made for sample P82, employing a graphite substrate to potentially slow the coupling of heat into the material and improve the melting of the metal to be coated. The first run using the graphite looked promising—no balls were formed but the surface was rough and uneven, with obvious dips and craters present. A second, separate pass at a rate increased by 50% to 15 mm/sec reintroduced the balls, with a decrease in adhesion to the substrate. Moving in the other direction, and slowing the powder rate to 6.3 mm/sec to hopefully heat the material more evenly, got rid of the balls again but resulted in a pooled appearance that was far from flat and uniform.

Sample P83 (Figure 5) was one of the best looking results obtained with aluminum on graphite. Going back to the original settings of  $5 \text{ kW/cm}^2$  and 9.78 mm/sec produced a good result on the first two passes (labeled run #1 on the right side of the sample in the figure). Very small balls were seen at the very edges of the tracks; but the surface was smoother, despite a slight “domed” appearance from center to edge of the run. Runs two and three attempted to preplace a thinner layer of metal, approximately  $1/64$ ”, and the result can be seen as a more pronounced ridge where the melt has pooled to the center and effectively wicked material away from the edges. As this appeared to be the best that could be achieved on graphite, a change in substrate was again called for on the next few runs.

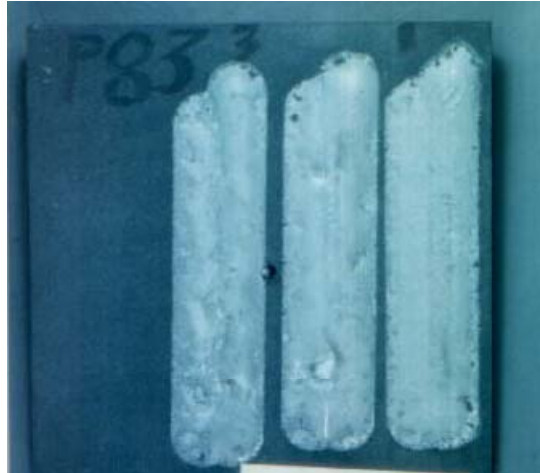


**Figure 5. Sample P83: Aluminum on Graphite.**

Sample P84 attempted to clad aluminum powder on an aluminum plate, hoping that similar metals with similar heat characteristics would result in a more uniform heat transfer and a more uniform coating. Two single-pass tests were performed, the second one at an elevated intensity of  $7.5 \text{ kW/cm}^2$ . Both runs showed the same formation of balls at the outer edges of the clad; however, the run at higher power gave finer pellets and what appeared as a clad coating below. Two runs of aluminum on graphite foil (P85) gave poor results, even with lower intensity (down to  $1.25 \text{ kW/cm}^2$ ) and faster translation speeds (12 mm/sec). These parameters were tried on the second pass to lessen the energy dumped into the thin material and avoid a burn-through problem encountered on the first pass. A test using a tungsten-bearing-resin material also was not very promising, as the clad coating induced some mechanical force on the substrate that resulted in the top layer of material being pulled off during sample cooling.

### **3.3.1.3 Reintroduction of Powder Feeder**

As an attempt to understand the reason for the formation of the aluminum b-b's, the method of powder delivery was examined. Through most of the previous tests with aluminum, the powder was placed by hand (preplaced) on the sample and then mechanically leveled to approximate a uniform layer that would be clad onto the substrate. The conclusions made were that while the powder layer appeared uniform it could not be assumed that variation did not exist from

test to test and that the starting conditions of the powder could be dependent on the person applying the prepositioned powder layer. If these nonuniformities had a role in the formation of aluminum pellets or in the wicking of the powder as the laser energy was applied, then having the powder already on the sample may not be the answer. The next two samples tested returned to the use of the powder feeder to spray the aluminum material into the laser beam at the time it passed over the substrate surface. Graphite was selected for this series, as it had the best looking result of all the substrates in the previous section.

For each of the five tests on the two graphite samples (P87 and P88), problems with the powder feed were encountered. While the use of the containment box and argon purge helped keep the mess from the powder spray to a manageable area, the actual delivery of the powder was still not as uniform as desired. Powder feed rates were varied ranging from 4 to 14 g/min, and the results went from no powder delivered (and burn-through of the substrate by the laser) to intermittent delivery to too much powder on the substrate and a very rough textured clad. It was determined that since the powder feed system seemed to work fine for the nickel-based alloys, physical differences between that material and the aluminum powder could be a cause. The aluminum powder is a great deal finer in particle size, and there was speculation that this could contribute to either clumping, clogging of the feed lines, or too much material passing through a nozzle that may have been intended or specifically sized for a larger-diameter particle. The manufacturer of the powder feed system was contacted, and a new nozzle was purchased to investigate its effect on the delivery of the coating material.

#### **3.3.1.4 Powder Feed Using Fine Powder Nozzle**

Nine tests were conducted using the newly purchased nozzle with the aluminum powder. The substrate samples were steel in order to step back to the substrate first used successfully with the “improperly sized” nozzle. Also, it was hoped that since there was little problem getting a quality coating of Versalloy 50 on steel using a nozzle appropriate for that alloy an equally good coating might be obtained with the nozzle sized for the finer aluminum powder. However, the

first three tests (P90) showed either a very poor coating quality or no coating deposited at all. During these tests, the same settings were used for the powder feed system using aluminum as those for the nickel-based alloy tests. It was then thought that perhaps the settings, in addition to the nozzle, needed to be changed with each new powder type. Upon contacting a representative at Sulzer Metco, alternate pressure settings were obtained for the vibration pressure in the powder hopper and for the feed pressure affecting the powder delivery. As can be seen in Figure 6, the test on the left side of sample P91 shows the reappearance of the fine b-b's of aluminum on the substrate surface. After slowing the sample translation speed by 30%, allowing more powder to reach the surface being irradiated, the result was even larger balls forming due to the increase in the amount of material accumulated. This can be seen on the right side of sample P91 in Figure 6.

Upon getting identical results on the first test using a new sample (P92), two questions were presented: (1) upon the observance of a flame coming out the beam entry hole in the top of the containment box, was it possible that the fine aluminum powder was being ignited by the laser beam and burned before it reached the substrate to be deposited as a uniform coating? and (2) was enough heat getting to the substrate due to this burning to melt the deposited material and prevent the pooling and ball formation that has been seen in several of the tests. Two single-pass tests were proposed, in opposite directions, in order to look at these questions. For the single pass shown in the middle of sample P92 (Figure 6), the powder was leading the beam, i.e., the powder was being deposited on the substrate prior to the laser beam's arrival. The same type of balls was formed but nearly as large as the second pass on the initial test (Figure 6, left side) for sample P92. This might indicate that too much material was present in the earlier runs. Since a second pass did not occur here, there was no opportunity for additional laser energy to be delivered to influence the formation of larger balls through any kind of pooling of material found in the "overspray" from the first pass. The third test on sample P92 (Figure 6, right side) involved the reversal of direction, making the beam lead the nozzle

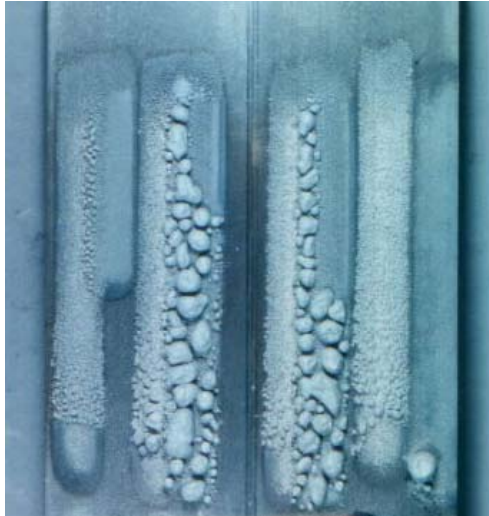


**Figure 6. Samples P91 (left) and P92 (right): Aluminum on Steel.**

depositing the powder on the surface. In this run, virtually no material was deposited. This result might have been expected, or at least understandable, since the beam had already passed over the spot where the powder was to be applied, giving little opportunity for the laser energy to interact with the powder and deposit the metal as a clad coating.

These tests, while not very successful in depositing an aluminum coating on the steel, did confirm that appropriate settings and orientation of the powder nozzle, sample translation direction, and laser beam delivery were being used.

#### **3.3.1.5 C-C Trials**

Before starting the trials on the C-C samples on the first day of this new set of experimental coating runs, two more tests were conducted using steel samples and employing a couple of additional modifications to the powder deposition system. The laser intensity for these tests was increased to  $7.5 \text{ kW/cm}^2$ , an increase to full power, to ensure that the powder and the sample were receiving enough heat to melt and adhere the coating to the substrate. With the increased power, there was concern that the effect of the powder overspray from the wide  $25^\circ$  nozzle would come back into the beam and cause flare-ups that could reflect some of the incident energy away from the sample. After the first tests (sample P94 and first run on P95), the nozzle was changed to  $0^\circ$  (straight bore), and the result appeared to be a very good looking coating.

This coating can be seen on the right side of sample P95 in Figure 7 and is estimated to be between 7 and 30 mils thick.

Since a lot of time and effort was expended just getting to the results achieved in testing sample P95, some caution was felt necessary before going into the five “program samples” provided by MLBC. Additional samples of C-C material that might be similar in properties were requested in order to practice and establish the optimum parameters for those final five samples. MLBC provided LHMEEL with a number of “scrap” samples of C-C that were left over from other programs. As such, these also varied in type, properties, and processing history. These samples would be good to practice on, but their own variety could show in different responses possible from sample to sample as well as with respect to the final samples that were the target for this effort.

The first few tests on the C-C substrates gave a wide range of results. This was seen in results such as a very heavy clad which exhibited cracking (P96) to no clad at all and a burned sample (P98). There was some concern, especially with the sample that had no deposit at all, that the nozzle was somehow getting clogged and not delivering a uniform (or any) stream of powder to the sample surface. For the next sample (P99, Figure 8), an increase in the powder feed and a lower laser power back to 5 kW/cm<sup>2</sup> was used to try to prevent any clogging that a weak pressure flow might create. On the first test, that adjustment may have overshot the mark, since there was a clad achieved, but there was also a return to the appearance of b-b's and pooling of the material in the center of the pass track. The second run adjusted the powder feed back to normal levels, and the result was much better. Some pooling or clumping of material was still noted, but the clad itself looked fully (continuously) coated over the diameter of the beam width.

One point to note about the scrap samples of C-C is that most of the individual pieces were different from all of the rest. That is, most of the samples differed in processing or composition from one another, influencing their properties, and making direct comparisons of results between individual tests rather difficult. This point is made now to preface introduction of the next sample

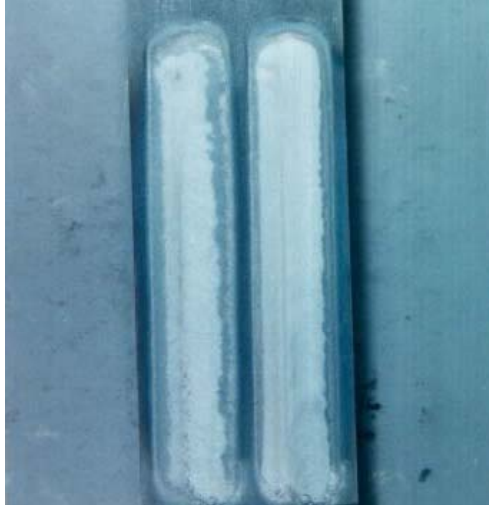


**Figure 7. Sample P95: Aluminum on Steel.**

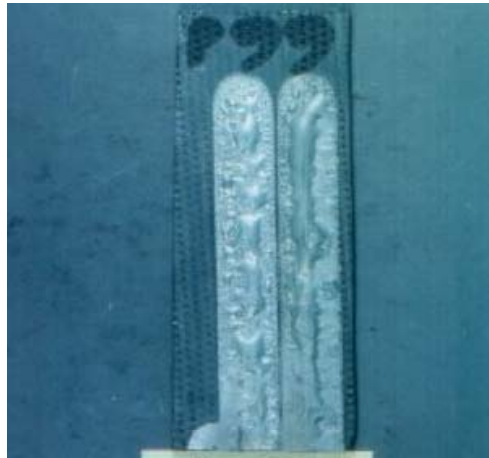


**Figure 8. Sample P99: Aluminum on C-C.**

tested (P100, Figure 9). For each of the three tests on this substrate, both the powder feed rate and the translation speed were increased to levels that eventually exceeded those for sample P98 in which no powder was deposited and the sample was burned. The results shown in the figure indicate one of the better coatings on C-C, even with the presence of random bumps of aluminum material in the center of the path. The clad deposited was thin to the point of borderline on the edges of the beam but continuous in appearance. The coating was thin enough that the texture of the substrate surface was still visible through the clad coating, and the bumps were not as large and continuous as the pooling

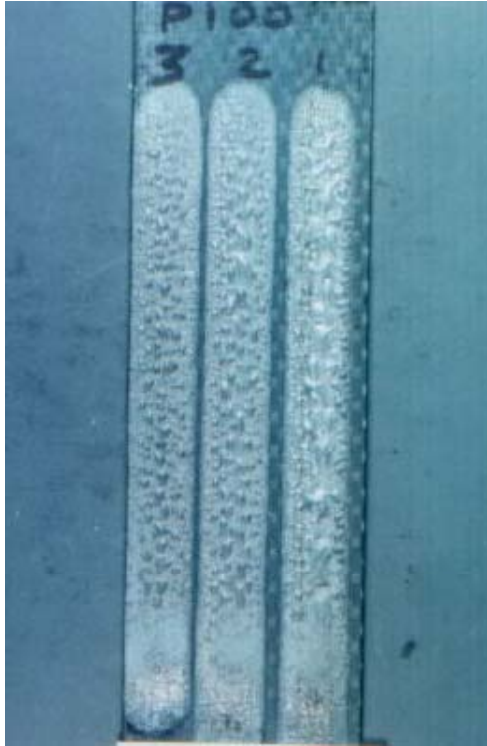


**Figure 9. Sample P100: Aluminum on C-C.**

and clumping experienced earlier. With confidence in the process and the results increased, the decision was made to move to a more specifically thermal plane material.

The initial sample (P101) of thermal plane material showed increasingly better results with each test. Four tests were made on this sample, with the translation rate increasing for the last two runs from 14.7 mm/sec to 18.3 mm/sec and the laser intensity increasing to 7.5 kW/cm<sup>2</sup> on the last shot. The increased speed seemed to help improve coverage on the outside edges of the path and lessen the size of the bumps formed in the clad material. The increase in power served to flow these bumps together, which in this case led to a more continuous and smoother clad coating with larger but thinner (flatter) bumps visible on the surface (Figure 10).

The next sample (P102, Figure 11) was basically the same kind of thermal plane material but a much larger sample piece size. This allowed for a longer length run for each individual test and the ability to do more tests per sample, as if there were multiple (10 in this case) sample substrates of the same material.

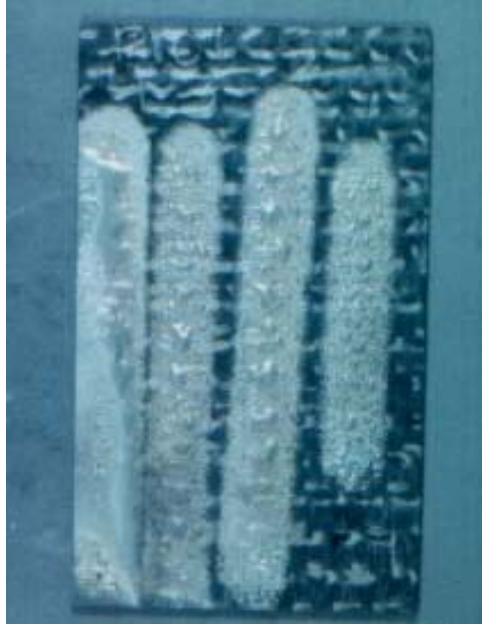


**Figure 10. Sample P101: Aluminum on C-C Thermal Plane Material.**



**Figure 11. Sample P102: Aluminum on Larger C-C Thermal Plane Material.**

The initial few shots looked much like that achieved on the previous sample, even as the translation speed was increased to 20.8 mm/sec and the power was increased to 9 kW/cm<sup>2</sup> by the third run. There was a noticeable flare-up of flame that became visible about halfway through the laser pass, beginning with the third test on this sample. It was thought that the higher energy laser beam was igniting the residual powder sprayed as it accumulated in the enclosure. From

the appearance of the clads, it might be that the heat from this short-lived flame was aiding in the melt of the coating, helping to smooth bumps and pools as the laser passed by. For tests 4 through 7, deposition parameter changes included slowing down the translation speed to 18.3 mm/sec, slowing the powder feed rate from 8 g/min to 3 g/min, increasing the powder-on time from 10 to 20 sec before opening the laser shutter, and reducing the power back to 7.5 kW/cm<sup>2</sup>. The intent of these changes was to insure full pressurization and stability of the powder feed system, a uniform delivery of coating material without too much excess, and the proper amount of heat needed to melt, but not burn, the powder being applied. The results over this series of tests showed no major changes in the clad appearance. The clads were fairly thin with some pooling of material evident, and a change in the melt pattern about halfway through the run nearly coincident with the appearance of the flare-ups mentioned earlier.

#### **3.3.1.6 Program C-C Sample Testing (Contractor's Samples)**

With all of the previously supplied C-C scrap samples now tested in various practice and evaluation runs, it was time for the contractor-prepared samples from MLBC. These samples were yet again different from those tested so far, even from the C-C samples on hand, as well as different from one another. There would only be opportunity for two to three tests per sample, as these were mostly smaller than the substrates available so far. This would again make these tests a "best effort" run based somewhat on the results and observations made during the testing done to date.

The first sample tested (P103) was a "very porous" sample of C-C. The results are shown in Figure 12 with the individual runs progressing from top to bottom in the photograph. A very high setting for the powder feed was used on the initial test (18 g/min) due to the porosity of the sample and the need to ensure that the pores would be filled with enough material to result in a continuous clad on the surface. The large dome of material in the center of the first run (Figure 12, top) indicated that possibly too much powder was deposited. Subsequent tests used rates of 15 g/min, 8 g/min, and 4 g/min. The second and third run showed a lessening in the size of the pooled material with a continuous clad



**Figure 12. Sample P103: Aluminum on Nondensified C-C.**

potentially beneath. The fourth test had insufficient powder supplied, which resulted in the burn damage to the substrate seen in the photograph.

Sample P104 (Figure 13) was an example of a very thin but 100% dense piece of C-C. The first test (Figure 13, left side) either had too much power for this thickness or not enough powder was distributed. The result was the burn-through shown and the additional burn damage surrounding the path of the run. For the second test, the power was lowered ( $5 \text{ kW/cm}^2$ ). Though no burn-through occurred, there was little damage effect to the substrate; but unfortunately there was still insufficient powder to deposit a coating. When the powder feed was increased, the coating on the right side of the sample resulted. The central region of the run looked good, but there were the familiar, yet smaller, bumps formed at both ends of the run. In addition, some of the clad material did penetrate the sample surface; and due to its thinness, it infiltrated the sample and was visible on the backside of the piece.

The next two samples (P105 and P106) were unique in that they were already infiltrated with aluminum, and both had been machined with cuts and grooves in the parts as they would appear for a specific component application. The first test on P105 (Figure 14, left side) was started at a lower laser intensity of  $5 \text{ kW/cm}^2$ , due to the infiltration effect seen on the nonaluminized sample just completed. Even at this lower power, the coating was not only deposited with pooling and the familiar balls evident but additionally had some of the aluminum already in the sample driven out the backside by the cladding process.

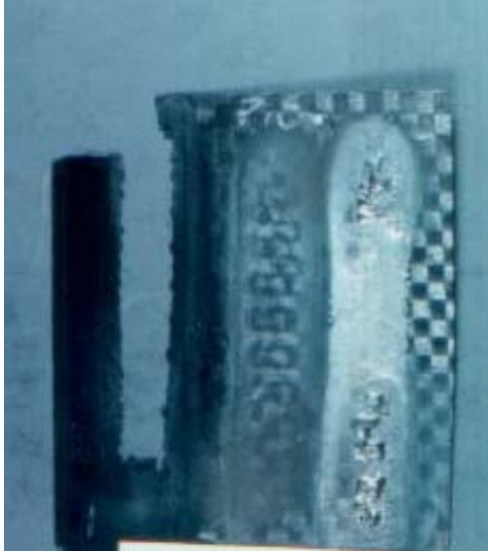


Figure 13. Sample P104: Aluminum on Thin, Dense C-C.

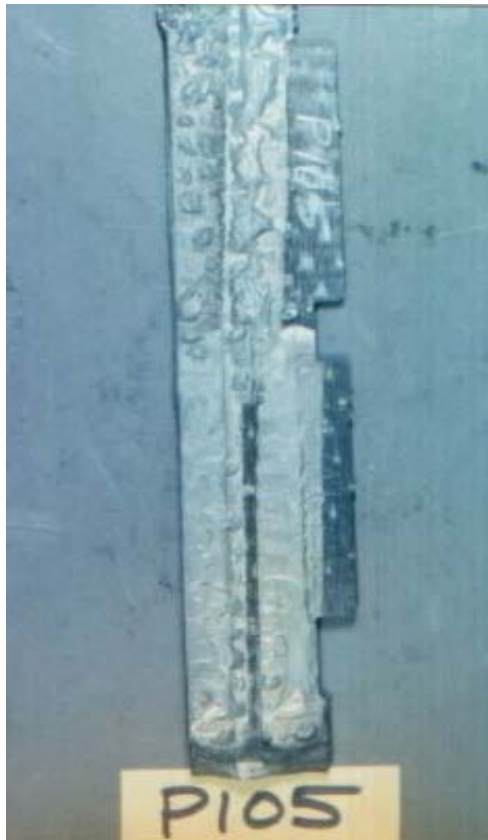
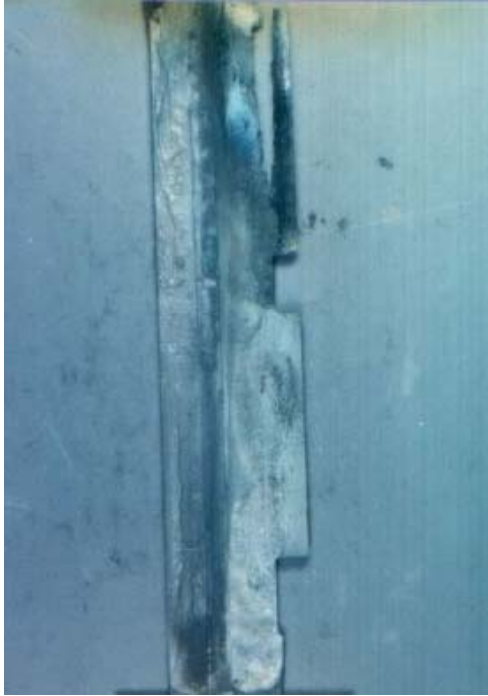


Figure 14. Sample P105: Aluminum on Aluminized, Machined C-C.

Increasing the laser intensity to  $7.5 \text{ kW/cm}^2$  gave larger but more interconnected pools on the surface and a smoother looking coating but also drove more of the internal aluminum out the back again. Lowering the powder feed rate to 4 g/min for the last two runs and the translation speed to 12.2 mm/sec for the last run on this sample gave a more uniform clad that was more completely filled and had fewer and smaller surface bumps present. The first test on sample P106 (Figure 15) was run at yet a slower translation speed (9.78 mm/sec) so that the slower powder feed could deliver enough coating to the sample to maintain a continuous coating. The coating appeared to be thicker but more uniform and smooth, so the rate was lowered one more time to 4.89 mm/sec for the next run. This gave a very thick coating to the point that it led to its cracking upon cooling. Since it appeared that too much powder was being dispersed for this slow of a speed, the feed rate was now reduced to a low of 2 g/min. This turned out to be the wrong move for this sample, as there was insufficient powder to melt at the increased laser power, resulting in the substrate getting too hot and burning near the end of the run. The effects of this damage unfortunately masked the good appearance of the first two tests on this sample, as can be seen in the photograph.

The final test of the series was on a piece somewhat related to the previous two, in that this was also an aluminumized piece of C-C. Sample P107 (Figure 16) was aluminum infiltrated but was not machined and had present what seemed an aluminum skin over most of the main surface of the part. The translation speed was increased so that dwell time of the laser was lessened and the feed rate increased so that the powder deposition could keep up with the increased speed of translation. However, even with these changes, the energy delivered by the laser was too much for the aluminum on the sample surface, resulting in the aluminum skin melting with no additional coating deposited and with some messy debonding of the pre-existing layer.



**Figure 15. Sample P106: Aluminum on Aluminized, Machined C-C.**

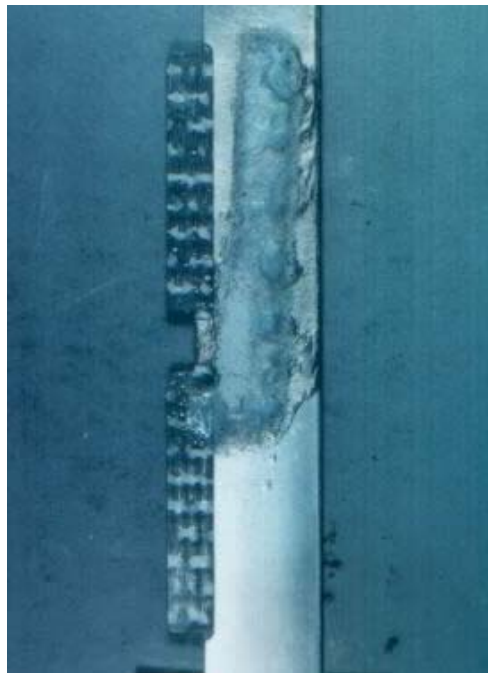


**Figure 16. Sample P107: Aluminum on Aluminized C-C.**

### **3.3.2 Test Review Meeting**

A meeting was held on 26 March 1999 to review the results of this experimental effort on the application of an aluminum coating. Mr. Hull and Mr. Bagford (Anteon) and Maj John Eric met with representatives from MLBC and their contractor, AMT. The testing program was reviewed with samples and photographs displayed to present the results and the findings to date. Some of the clad samples were provided to UDRI for further analysis, including determination of coating quality, bond strength, and effect on the substrate. Despite the mixed success in getting a coating clad on these varied substrates, all parties were pleased with the results and the information gained from them.

### **3.3.3 Initial Micrographic Review of Selected Samples**

Samples P100, P102, P105, and P106 were sectioned by Dr. Dave Anderson of UDRI for inspection of the interface between the clad metal coating and the C-C substrate. Maj Eric and Dr. Anderson initially met on 10 May 1999 to view the samples directly with the microscope and receive Dr. Anderson's assistance and expertise in determining the success of the coating effort as indicated by the quality of the interface between the materials. The microscope used bright field and fluorescent illumination and magnified the field 400 times.

Sample P100 was one of the better looking samples (XN-50?) that was obtained from MLBC's scrap supplies. Referring back to Figure 9, run 100-1 when viewed through the microscope showed cracks evident in the C-C material but not between the metal and the C-C, indicating the presence of a good bond. This was commented as being a very good coating in terms of metal deposition and the good interface. Run 100-2 showed some cracks also but was very similar to the first run. The final run, as indicated in the testing comments, was thin, especially on the edges of the beam path. There was metal present on the surface, but it was not continuous. The metal that was deposited showed good adherence in spite of the lack of obvious mechanical interlocks with the carbon substrate.

Sample P102 was the larger piece of thermal plane material (K-321?) that was used for ten cladding runs. This sample was illustrated in Figure 11. Due to the size of the sample, the part was sectioned and then cut into two parts, so as to fit more easily into the mounting piece. Runs 1 through 5 were presented in reverse order according to the way that they were seen on the video screen, and runs 6 through 10 were presented next. Run 102-5 showed that the aluminum, as nice as it looked on the surface, was just lying on the substrate. There was potting resin clearly visible between the metal and the carbon when viewed under fluorescent conditions, indicating that the aluminum did not penetrate the carbon and is not adhering well to the substrate surface. Run 102-4 showed a large bubble (void) at one edge, indicating a separation between the metal and the carbon. Voids and cracks were visible in the C-C substrate. The three initial runs on this sample, 102-1, 102-2, 102-3, all showed lack of adhesion of the metal to the carbon. There were some visible separations at the interface and some minor evidence of metal penetration but to a very shallow depth. Runs 102-6 and 102-7, which used a lower powder feed rate and showed a change in the clad appearance halfway through the run, did not really show much coating at all under the microscope. What was there was very fragmented and not at all continuous. Runs 102-8 and 102-9, which used a higher powder feed rate and lower laser intensity than the previous two runs, did get more metal to adhere to the carbon. While gaps were still present, there was more metal penetration and some evidence of good mechanical adhesion when viewed under magnification. The view of the final run confirmed that the coating material did not spread; rather it pooled in the center of the laser's path.

P105 was the first of the aluminized C-C, machined samples to be tested. (Figure 14) There is much porosity in the C-C, and the aluminum can be seen all the way through the material. This would include the metal already present from the aluminization as well as metal from the coating attempt. Some voids were visible in the substrate that were not even penetrated by the potting resin. With regard to these voids and to the aluminum that was apparently driven out during the cladding process, these pockets may not have been filled by the

manufacturing process. Subsequently, trapped gasses expanding under laser heating of the sample may have caused some of the aluminum to be driven out the backside of the carbon.

The other aluminized sample, P106, showed indications that the coating was able to clad around cut edges well. Subsurface cracks on the order of 100  $\mu\text{m}$  were observed, and regions of the substrate around burned sections showed large bubbles and voids.

### **3.3.4 Summary Micrographic Data Review**

After the initial view of sectioned samples under the microscope, Dr. Anderson provided additional photographs of some of the more prominent features from these samples. Subsequently, Mr. Hull and Maj Eric met once more with Dr. Anderson to review the photographs and discuss the sectioned samples. The photographs were reviewed as well as a paper printout (at 200X) of a photo-mosaic of the sectioned interface for each of these four samples. Additional information and observations were added to those already presented from the initial viewing of the samples.

The P100 sample was most likely a pitch-based fiber and has a potential for high thermal conductivity. It was also noted that for run 100-1, there is a crack about one fiber width below the surface in the substrate material (Figure 17). This may be due to stresses created during the aluminum cooling process or resin shrinkage, which is normal for a matrix-rich region.

The P102 sample was most likely a PAN-based fiber. Commenting on the photographic data for run 102-1, cracking is evident at the metal-carbon interface. Some of the subsurface cracks were found to be filled with fluorescent material, which would lead one to conclude that there must also be cracks present in the metal clad itself. Figure 18 shows the separation of the metal clad from the substrate, while Figure 19 shows some of the penetration into the substrate that the metal coating was able to achieve.

Figure 20 shows the clad coating over one of the cut features in sample P105. This was one of the aluminized, machined samples that was from the

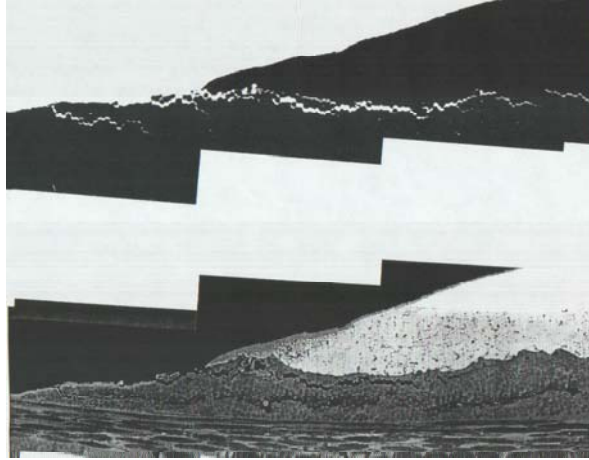


**Figure 17. Cracking Below Surface of Sample P100, Run #1.**

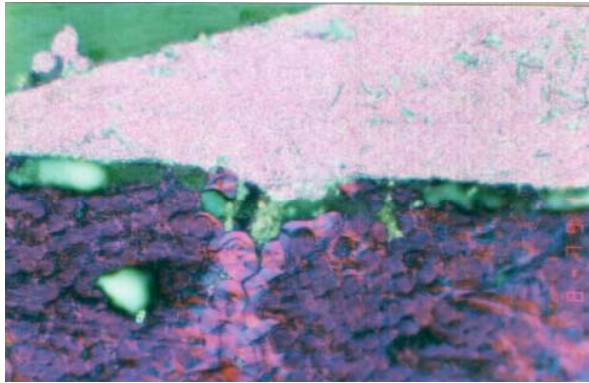


**Figure 18. Aluminum/C-C Interface on Sample P102, Run #1.**

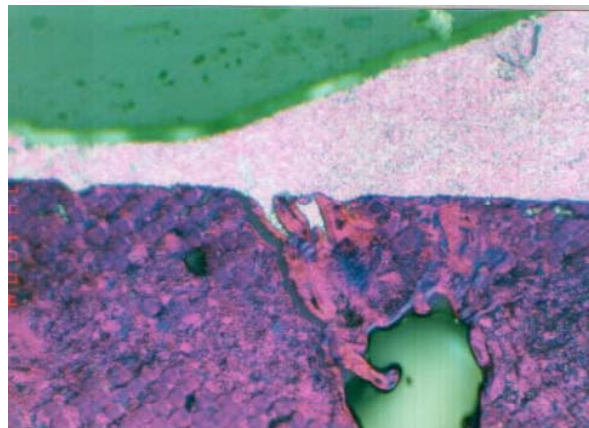


**Figure 19. Aluminum Penetration Into Surface of Sample P102, Run #1.**

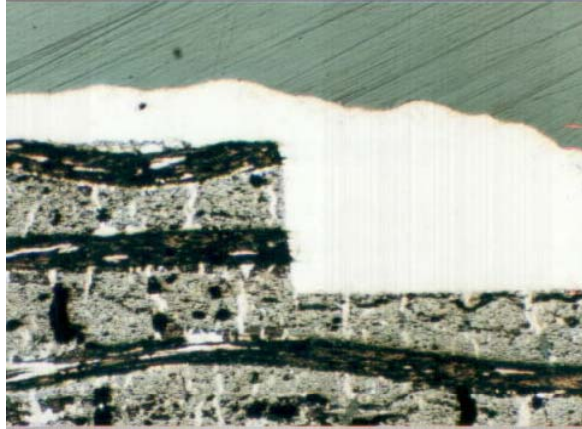


**Figure 20. Aluminum Clad Follows the Machined Features on Sample P105.**

MLBC contract program. Good adhesion is apparent from the photographs, and there was not much fluorescent resin penetration below the surface of the substrate. The light areas in Figure 20 show the aluminum that was already present that created the aluminization of the carbon sample. This aluminum almost entirely makes up the matrix material for the carbon fibers.

Figures 21 through 23 show the clad coating forming around the cut edge on sample P106. The aluminum material does seem to be mechanically anchored to the substrate, adding strength to the coating. There appeared to be less aluminum present initially, as more voids seem to exist in the photographs. This could be where the initial aluminizing material was present but was forced out during the cladding process and not replaced with aluminum material used for the clad coating.

### **3.3.5 Series 2—Tests on a Common C-C Substrate**

As mentioned earlier in the report, about a year after the first series was run, a second series of experiments was scheduled in the LHMEEL facility. This series sought to use a known, pedigreed sample for the coating substrate and to eliminate some of the variation that resulted from so many and varied types of substrates previously obtained. The sample used for this series was not available during the first series but resulted from samples delivered on a contract being completed for MLBC. MLBC made a couple of C-C panels available to this

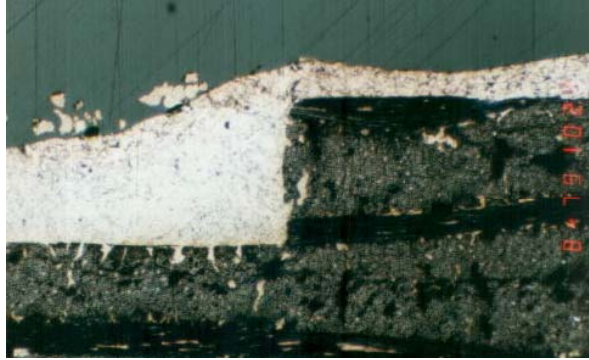


**Figure 21. Aluminum Clad Over a Machined Feature on Sample P106.**

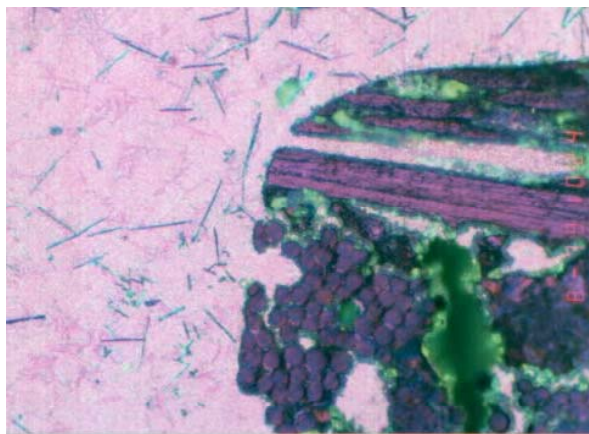


**Figure 22. Aluminum Cladding on a Machined Feature on Sample P106.**

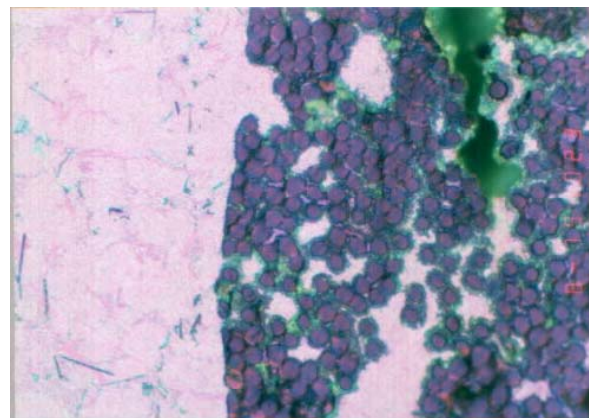


**Figure 23. View Further Down the Side of Figure 22 Feature (P106).**

test series; and with the assistance of MLBC's on-site UDRI technical staff, these were prepared for cladding and then subsequently sectioned for microscopic examination.

#### **3.3.5.1 Nickel on Steel Substrate**

For the first coating run of this new series, a nickel chromium alloy was deposited on a 1018 carbon steel substrate. This served to again provide a means to ensure the cladding system was setup and working properly. This was the primary materials combination used in the previous chromium replacement project and served as a common starting point for both test series. In addition, this gave a benchmark comparison of an ideal "same-year" cladding sample for the rest of the runs on the carbon composite. This can be seen in Figure 24.

#### **3.3.5.2 Nickel on C-C Substrate**

The first attempts at coating the nickel alloy on the carbon sample gave a similar result to what we had experienced with coating powdered aluminum. That is, the metal showed pooling, or small bump formation, that prevented a uniform coating from being deposited. It appeared as though the surface tension of the metal was too great under these conditions to allow complete wetting of the surface to be coated. A series of runs were performed that employed the application of a soldering flux, containing ZnCl, over the surface of the substrate, and these showed some improved results. On multi-pass runs, it was also noted that there might be some direction dependence on the quality of the coating. As the substrate is translated beneath the powder nozzle, the incident laser heats the powder and the substrate. In one direction, the substrate is moving toward the powder stream. On the return pass, it moves away and seems less affected by the powder jet blowing the powder out of the laser beam spot before it can be clad to the surface. Relatively good results were achieved using a combination of these measures: precoating the substrate surface with the soldering flux, applying a prepositioned layer of powder on the surface without use of the laser, and single-direction rastering of the laser beam in several passes until the substrate is covered. An illustration of this is shown in Figures 25 and 26.



**Figure 24. Nickel Chromium Alloy Clad on Steel.**



**Figure 25. Nickel Alloy Cladding Using Bi-directional Passes.**



**Figure 26. Nickel Alloy Cladding Using Single-Direction Rastering.**

### **3.3.5.3 Alumina on C-C Substrate**

This series of cladding runs made the switch from a metal powder to a ceramic in the form of gray alumina powder for the coating material. The use of this material, it was lighter and finer than the nickel alloy, did confirm the directional dependence of the cladding for these materials. It appears that on the return passes the material is blown out of the way of the laser beam spot. In some cases, ridges of material were deposited only on the edges of the deposition path, possibly due to blow back of powder during the process. This material was successfully coated on the C-C. The average thickness of the coating was about 5 mils, and did not seem to vary much even when two passes were made over the same deposition path. Rather than doubling the coating thickness, the measured thickness increased only about 50%. The thicker coatings, whether produced by an increase in the powder feed rate or by a double pass cladding, did display some brittleness and cracking. These thicker coatings did not appear to adhere very well to the substrate and were rather easily chipped off or dislodged by the tip of a pencil. The alumina ceramic, however, did demonstrate that it could be uniformly deposited in adjacent paths with little effect from overlap of powder. The result of one of these cladding tests is shown in Figure 27.

### **3.3.5.4 Magnesium Oxide/Zirconium Oxide on C-C Substrate**

The quality of coating clad with this ceramic material was far different than that experienced with the alumina powder for this C-C composite. There was very little, if any, material deposited on any of the samples attempting to be clad with the magnesium oxide/zirconium oxide powder. The coating was very brittle and was easily removed from the substrate surface. Even with as little mechanical pressure as was applied with a soft-bristled brush that we used for removing excess powder, some of the larger agglomerations of the ceramic showed little adhesion to the composite substrate. Even such measures as employing the previously described flux material or coating this material over a layer of the nickel alloy clad onto the carbon did not help in obtaining an improved coating. In some cases, the powder appears to be burning off before it



**Figure 27. Gray Alumina Cladding on C-C Using Single-Direction Passes.**

has a chance to become clad to the substrate. Figures 28 and 29 illustrate the results found with this material.

### **3.3.6 Discussion of Series 2 Preliminary Results**

From a visual inspection of the coatings deposited, there was a wide variety in the results achieved among the three powdered materials used in this test series. By far the best looking coating was that deposited with the alumina on the C-C substrate. Pure  $\text{Al}_2\text{O}_3$  has a thermal expansion coefficient of  $6.5 \times 10^{-6}/^\circ\text{K}$ , which is close to that for SiC ( $5.3 \times 10^{-6}/^\circ\text{K}$ ), a material that is often used to coat C-C. The laser was able to heat the alumina well above its melting point, and a uniform coating was applied that fully filled the beam spot. The material was also demonstrated to be able to be coated over itself and other previously deposited materials without adverse effect to either the substrate or any previous coating layer. The next best coating was produced by the nickel chromium alloy powder. Several depositions showed that the material could be coated continuously on the C-C. The coatings in these cases filled the beam spot and appeared to be uniform in the area covered. However, in many instances this material also displayed a coating surface that varied from mildly to very bumpy in appearance. It is apparent that either a preliminary substrate surface preparation, some degree of post-processing machining/polishing, or a combination of both may be necessary to obtain a smooth, continuous coating layer on substrates such as C-C. NiCr 80/20 is advertised as a good bond coat for ceramics and a good corrosion protection material with good machinability.<sup>6</sup>



**Figure 28. Magnesium Oxide/Zirconium Oxide on C-C Substrate.**



**Figure 29. Edge View of the Sample Shown in Figure 28.**

This was demonstrated when the alumina powder was also successfully coated over a C-C substrate that had already been clad with a layer of the NiCr powder. As can be seen in Figure 30, the ceramic coating is uniformly coated within the laser cladding path over the metal layer, without degradation to the previous coating or the substrate. The bumps visible in the coating are those that previously existed from the NiCr cladding and were overcoated and enhanced by the alumina coating. The third material attempted,  $ZrO_2/MgO$  powder, was not successfully coated and is not recommended as a candidate coating material for C-C applications. Its melting point is significantly higher than the other two materials, approaching  $4000^\circ F$ , and may not have been fully melted by the laser. The  $4000^\circ F$  measured in the lab for the laser spot was on a bare substrate where no powder had been applied. It demonstrated a value that may have been reduced during an actual cladding run by reflection of laser energy by the presence of the powder stream.



Figure 30. Alumina Powder Clad Over NiCr Alloy on C-C Substrate.

### **3.3.7 Summary Discussion of Micrograph Results**

From the discussion above, the best outwardly looking coating was that of the alumina deposited on the C-C substrate. Its micrograph is shown in Figure 31.

The views in Figure 31 show two locations from the sample depicted in Figure 27. The left side of the picture is shown in bright field, while the right is the corresponding location under fluorescence. The coating itself appears to be well bonded to the substrate, as no interface separations that would have been infiltrated by the potting resin are visible. A couple of significant cracks do appear that penetrate the coating from the surface to the substrate, as highlighted by the right-side views in the figure. While they do penetrate the surface, they do not appear to have affected the substrate or started a separation of the coating at the coating-substrate interface.

The next micrograph of interest, shown in Figure 32, is for the NiCr alloy clad on C-C. The sample depicted here is that shown in Figure 26. The top row of photos in Figure 32 is a composite view of several of the bumps of alloy material that formed as a result of the cladding process. It is even more evident in these photos that a continuous, uniform coating was not always achieved and was not always as good as it appeared to the naked eye. The photo in the lower right is a segment of the composite photo, specifically the large bump of alloy material from the far-right end, enlarged to 100X for more complete viewing of the material clad. In addition to the evidence of pores in the coating material, as shown by the dark spherical voids in the coating, the material itself is only

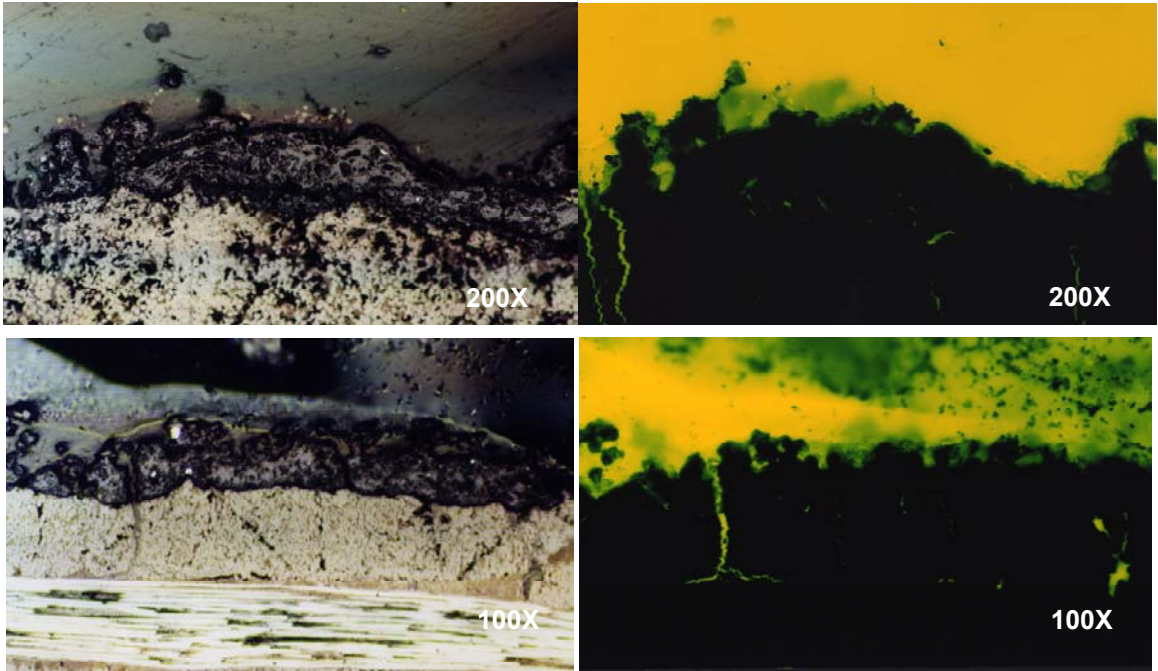


Figure 31. Micrograph of Alumina Cladding on C-C Substrate.

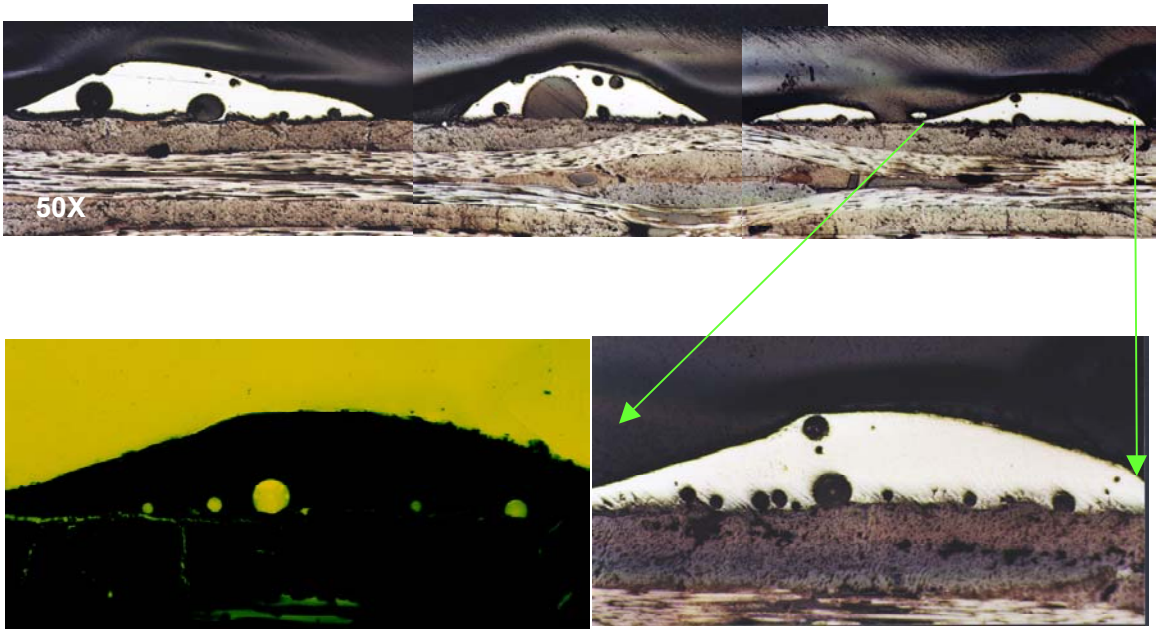
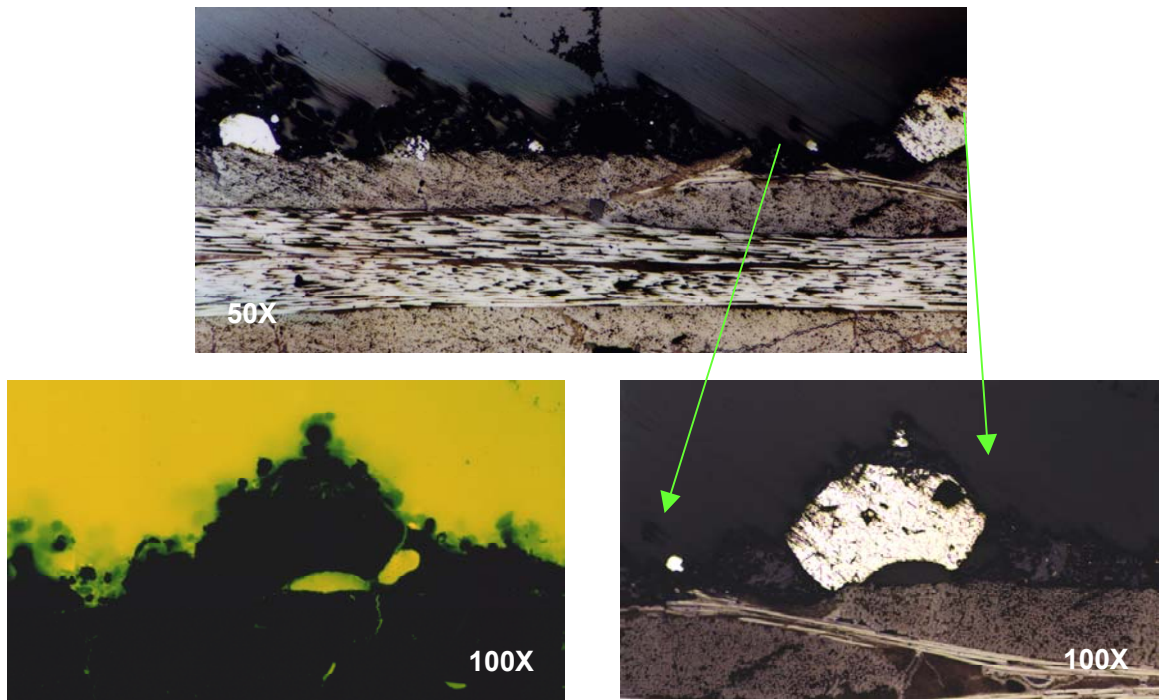


Figure 32. Micrograph Showing NiCr Alloy Clad Over a C-C Substrate.

partially adhered to the composite substrate. This second observation can be seen in the view under fluorescence, where a thin crack at the interface between the coating and the substrate is shown via the resin infiltration on the left side of the coating view.

The final micrograph of interest is the views, in Figure 33, of the sample depicted in Figure 30 that had a second cladding run deposit an alumina coating over a previously clad layer of NiCr alloy. As can be seen in the photos, the alumina layer did follow the contours of the alloy-cladding layer already present. While both layers might not be completely continuous, it is evident that the alumina did adhere to the NiCr alloy and the C-C, with very little separation at the interface visible. The second cladding run did not degrade the first layer of the NiCr any worse than it already was; the same bump formations that are visible in Figure 32 are also visible in Figure 33. Voids are still present, with the addition of the second layer of alumina not appearing to penetrate into these spaces, as the resin reveals in the view under fluorescence in the lower left of the figure.



**Figure 33. Alumina Cladding Over a NiCr-Clad C-C Substrate.**

## 4.0 SUMMARY

These test series were mainly intended to explore and demonstrate the feasibility of laser cladding as a deposition process for oxidation protection materials on C-C. The testing performed during the reporting period was very useful in determining and demonstrating some of the issues that may play a role in the process of coating a metal or a nonmetal onto a C-C substrate. The materials obtained for the test were those that were either on-hand in the laboratory or were easily obtained without major lead times in delivery. The cladding runs were performed as a best-effort attempt to investigate the potential for various classes of material to be deposited in this fashion and to illuminate some of the issues that may affect the ability to coat onto C-C. While the results were mixed and dependent on the characteristics of the substrate as well as the coating material, much was learned of the interactions that have to occur to produce a quality coating. While surface appearance is a factor in the determination of success in the coating process, it was also seen that other means, such as micrographic analysis, can give a different view of the quality of the end result. These tests have shown that certain ceramics can be coated successfully and even some metals may do reasonably well. Materials selection processes may indicate that other materials not tested here would be better candidates for the oxidation protection application; however, more investigation remains to be done in this area. Process parameters such as sample translation speed, powder rate, substrate surface preparation (use of flux materials, preheating or precoating), post-process machining, or polishing may all individually affect the way that a coating material is applied. In the end, the laser cladding process does present an option as an economical; simple; and, in many cases, effective way to deposit a powdered coating material onto composite substrates.

## **5.0 REFERENCES**

1. Sulzer Metco Type 4MP Powder Feed Unit Instruction Booklet, Instruction G 38851, Model 851, Cat. No. 4MP 111, Sulzer Metco Inc., Westbury NY.
2. Letter Correspondence, HITCO Carbon Composites, Inc., 17 September 1999.
3. Sulzer Metco Materials Safety Data Sheet, No. 50-112, Rev. 6, Sulzer Metco Inc., Westbury NY, 10 November 1997.
4. Sulzer Metco Materials Safety Data Sheet, No. 50-134, Rev. 7, Sulzer Metco Inc., Westbury NY, 14 October 1996.
5. Sulzer Metco Materials Safety Data Sheet, No. 50-150, Rev. 6, Sulzer Metco Inc., Westbury NY, 9 May 1996.
6. "AMPERIT (reg.) Thermal Spray Powders," H.C. Starck, Available: [www.hcstarck.de/gb/keramik/b\\_keramik\\_3c\\_e.htm](http://www.hcstarck.de/gb/keramik/b_keramik_3c_e.htm), 11 May 2000.